Published online 20 April 2017

Nucleic Acids Research, 2017, Vol. 45, No. 20 ***e167***
doi: 10.1093/nar/gkx260

Bidirectional approaches for optogenetic regulation of gene expression in mammalian cells using *Arabidopsis* cryptochrome 2

Gopal P. Pathak[1,†], Jessica I. Spiltoir[1,†], Camilla Höglund[2], Lauren R. Polstein[3], Sari Heine-Koskinen[2], Charles A. Gersbach[3], Jari Rossi[2] and Chandra L. Tucker[1,*]

[1]Department of Pharmacology, University of Colorado School of Medicine, Aurora, CO 80045, USA, [2]Department of Anatomy, Faculty of Medicine, University of Helsinki, Helsinki, Finland and [3]Department of Biomedical Engineering, Duke University, Durham, NC 27708, USA

Received October 05, 2016; Revised March 13, 2017; Editorial Decision April 03, 2017; Accepted April 17, 2017

ABSTRACT

Optogenetic tools allow regulation of cellular processes with light, which can be delivered with spatiotemporal resolution. In previous work, we used cryptochrome 2 (CRY2) and CIB1, *Arabidopsis* proteins that interact upon light illumination, to regulate transcription with light in yeast. While adopting this approach to regulate transcription in mammalian cells, we observed light-dependent redistribution and clearing of CRY2-tethered proteins within the nucleus. The nuclear clearing phenotype was dependent on the presence of a dimerization domain contained within the CRY2-fused transcriptional activators. We used this knowledge to develop two different approaches to regulate cellular protein levels with light: a system using CRY2 and CIB1 to induce protein expression with light through stimulation of transcription, and a system using CRY2 and a LOV-fused degron to simultaneously block transcription and deplete protein levels with light. These tools will allow precise, bi-directional control of gene expression in a variety of cells and model systems.

INTRODUCTION

Systems for conditional control of transcription provide a powerful means to interrogate the functions of individual transcription factors and the roles of regulated transcriptional programs. Chemically-regulated systems such as Tet-OFF and Tet-ON, which allow blockage or induction of transcriptional activity with the addition of a small molecule, have been widely used for inducible regulation (1,2). Although chemical systems provide tight control of transcriptional activity, they have limited spatial resolution and the chemicals can be difficult to remove. For example, Tet-system regulators such as doxycycline can bind non-specifically to cells or cell matrix components, requiring multiple washes or cell replating to completely remove the compound (3). Recently, light-regulated systems have been developed that overcome some limitations of chemical systems. The first system allowing light control of transcription, involving use of a plant photoreceptor interaction to bring together a split Gal4 transcription factor, was developed over a decade ago in yeast (4). Since then, a variety of systems based on engineered or natural light-sensitive photoreceptor proteins have emerged for use in higher eukaryotes (5–12). While existing systems are being broadly adopted, efficacy and background vary considerably in different organisms and cell types, with no single system showing ideal properties across all applications.

Cryptochrome 2 (CRY2) and CIB1 are *Arabidopsis* proteins that dimerize upon exposure to blue light (13,14). Previously, we used these modules to develop a system to regulate transcription in yeast, using blue light to reconstitute a split transcription factor through CRY2–CIB1 binding (14–16). Attempts by our group or others (7,8,17) to adapt this system for transcriptional control in higher eukaryotes have suffered from poor light-stimulated activity or high basal activity in dark. While our original system in yeast fused CRY2 to a DNA binding domain and CIB1 to an activation domain, other studies fused CIB1 to a DNA binding domain (8,17). Because CIB1 is itself a transcriptional activator (7,13), the CIB1-BD fusion can activate transcription on its own without CRY2–CIB1 association, and thus can result in increased dark background activity.

In this work, we set out to determine why the split transcription approach we initially developed, which functions well in yeast, has not been successful in mammalian cells. Unexpectedly, we find that in mammalian cells, CRY2-BD fusion constructs used in the split transcriptional system

*To whom correspondence should be addressed. Tel: +1 303 724 6337; Fax: +1 303 724 3663; Email: chandra.tucker@ucdenver.edu
†These authors contributed equally to this work as first authors.

undergo clustering and clearing in the nucleus in the presence of light. This observation led us to engineer two powerful new systems allowing conditional control of gene expression levels in opposite directions with light: one allowing induction of transcription with light with low background and high dynamic range, and a second allowing light-dependent reduction of protein expression. These new tools complement the existing toolkit of chemical and light-regulated systems for conditional regulation of gene expression.

MATERIALS AND METHODS

Constructs

Construct sequences are provided in Supplementary Table S2. GalBD-CRY2 (B689) and VP16-CIB1 (B692) were PCR amplified from yeast two-hybrid plasmids (14,15) and cloned into pCMV-Gal4 (Addgene 24345) after removing Gal4 by Kpn I/Not I digestion (for GalBD-CRY2) or Kpn I/Age I digestion (for VP16-CIB1). CRY-GalVP16 (B695) was generated by digesting CRY2-CreN (14), containing CRY2(+NLS) downstream of a mCherry-IRES sequence, with Not I and Xma I to remove CreN, and inserting a 573 bp fragment of Gal4BD-VP16AD (also digested at Not I/Xma I sites) containing residues 413–454 of VP16. To generate CRY(ΔNLS)-mCh-tTA (B714), tTA2 (from pBT224_(pCA-tTA2), Addgene 36430) was amplified by PCR and inserted into CRY(ΔNLS)-mCh (14) at Bsr GI/Not I sites. The galUAS-luciferase reporter was pGL2-GAL4UAS-Luc (Addgene 33020); the tetO-luciferase reporter was pTRE3G-luciferase (Clontech).

CRY-GalΔDD-VP16 (B1012) is equivalent to CRY-GalVP16 but missing residues 66–95 of the Gal4 binding domain (comprising the majority of the dimerization domain). To generate this, a first fragment containing Gal4BD residues 1–65 and an engineered 'SR' linker containing an Xba I site, and a second fragment containing Gal4BD residues 96–147 through the end of VP16 were amplified, then joined by overlap extension PCR. The GalBD(Δ66-95)-VP16 PCR product was ligated into B695 (CRY-GalVP16) at Not I and Xma I sites. GalVP16 (B1018) and GalΔDD-VP16 (B1019) were generated from B695 and B1012, respectively, by digesting with Not I and Sal I to remove the CRY2 fragment, followed by blunt end fill-in with T4 DNA Polymerase and ligation. To generate CRY-dsRed-GalΔDD-VP16 (B1017), flanking Not I sites were added to dsRed by PCR, and this fragment was ligated between CRY2 and Gal(ΔDD) at the Not I site of GalBD(Δ66-95)-VP16.

CRY-Gal(1–65) (B1013) contains a fusion of CRY2 with Gal4(1–65), and was cloned by digesting CRY-Gal(ΔDD)-VP16 with Xba I and Sma I to remove Gal4(96–147) and VP16, blunt end fill-in with T4 DNA Polymerase, followed by ligation. CIB1-VP16-CIB1 (B1015) was cloned by amplifying CIB1 using PCR to add flanking Kpn I sites, then ligating this fragment into B692 (VP16-CIB1) at a Kpn I site N-terminal to VP16. CIB1-VP16 (B1014) was generated by amplifying CIB1-VP16 from CIB1-VP16-CIB1 using PCR, then ligating into pcDNA3.1+ at Eco RV and Xba I sites. CIB1-VP64 (B1016) was cloned by removing CreC in the plasmid CIB1-CreC(N1) (18) (Addgene 75367) at Bsp EI and Bsr GI sites and replacing with a SV40 NLS-VP64 fragment amplified from pcDNA-dCas9-VP64 (Addgene 47107).

To generate CRY-GalVP16l (B694), first mCherry was removed in the construct CRY(ΔNLS)-mCh (14) (cut with Xma I/Not I) and replaced with the Gal4 DNA binding domain (residues 1–147). Next, a fragment containing residues 1–147 of Gal4 DNA binding domain, a glycine–serine (G–S) linker, then the VP16 activation domain (residues 413–490) was inserted at Bsr GI-Not I sites to generate CRY-GalVP16l. To generate CRY-tTA (B702), CRY2(ΔNLS)-mCh (14), containing CRY2 with a mutated NLS sequence in the pmCherryN1 vector (Clontech), was digested at Xma I and Not I sites to remove mCherry, and replaced with tTA from pBT224_(pCA-tTA2) (Addgene 36430) digested with Xma I and Not I. CRY2olig(FL)-tTA (B703) was generated by inserting full length CRY2olig (E490G CRY2ΔNLS) between the Xho I and Xma I sites of CRY-tTA. CRY2-dCas9-VP64 was cloned in the backbone pcDNA3.1 using Gibson Assembly. The dCas9 fragment was amplified from pcDNA3.1-dCas9-VP64 (Addgene 47107) using the primers 5′-GAAACGCAAA GTTGGGCGCG CCCGCGGAAT GGATAAGAAATACTC-3′ and 5′-CGTCCAGCGC GTCGGCGCGC CCAACTTTGC GTTT-3′ and cloned into pcDNA3.1-CRY2FL-VP64 (Addgene 60554) at the Pac I site.

pGL2-*GalUAS*-GFP-HA (B1007) contains GFP (GFPuv variant) followed by the nuclear export signal (NES) of Id1 (amplified from GFP-Id1NES by PCR) inserted at Hind III/Eco RI sites into *pGL2-GalUAS*-Luc (Addgene 33020). A HA epitope was ligated in frame after GFP at Avr II/Cla I sites to yield pGL2-*GalUAS*-GFP-HA. pGL2-*GalUAS*-GFP-LOVdeg (B710) is in the same backbone, and contains GFP-NES followed by a LOV-degron sequence (PCR amplified from pBMN HAYFP-LOV24, Addgene 49570) inserted at the Bsr GI site at the C-terminus of GFP. The *CMV*-GFP-LOVdeg construct (B711) was generated by inserting the GFP-LOVdeg fragment from pGL2-*GalUAS*-LOVdeg into the pcDNA3.1 backbone after the CMV promoter (Hind III site).

Cell culture and light treatment conditions

HEK293T cells were maintained in Dulbecco's modified Eagle medium (DMEM) supplemented with 10% FBS at 37°C with 5% CO_2. HEK293T cells were transfected using calcium phosphate or Lipofectamine 2000 or 3000 (Invitrogen), according to the manufacturer's protocol. Cells were transfected with 1 μg DNA for each construct (for experiments in 12-well plates) or scaled up accordingly for larger plates. DNA was transfected at a ratio of 1:1 (two constructs, 2 μg total DNA per well), 1:1:1 (three constructs, 3 μg total per well) or 1:1:1:1 (four constructs, 4 μg total DNA). Nonspecific 'stuffer' DNA (for example, pmCherry-N1 empty vector) was included in transfections as needed to ensure all transfection wells contained equal amounts of DNA. Dark samples were wrapped in aluminum foil immediately after transfection. Light-treated cells were illuminated using a custom programmable blue LED light source (461 nm, 7.4 mW/cm^2). Pulse length and interval used was 2

s pulse every 3 min for all experiments (1.1% duty cycle), unless differently indicated. Light dosage experiments shown in Figure 3F used a custom built LED light source designed for 24-well plates and low illumination levels (19) and used constant blue light rather than pulses.

Luciferase assays

Measurement of luciferase activity (Fluc) was carried out using the Luciferase Assay System (Promega) according the manufacturer's protocol. A Modulus microplate reader (Turner Biosystems) was used to quantify luminescence. Fluc activity was normalized using a cotransfected RSV-lacZ control in which ß-galactosidase activity was determined using an ONPG assay (Clontech Laboratories, protocol #PT3024-1) using *o*-nitrophenyl-β-D-galactopyranoside (Thermo Scientific) as a substrate. Fluc/lac activity is represented as fold increase over a control containing only the luciferase reporter.

Quantitative RT-PCR

Total RNA was prepared using TRI reagent (Molecular Research Center) following the manufacturer's protocol. RNA was verified by calculation of OD280/260 ratio using an Eppendorf spectrophotometer. To remove genomic DNA, total RNA was treated with RQ1 RNAse free DNAse (Promega). High Capacity cDNA Archive Kit (Applied Biosystems) was used to synthesize cDNA from DNAse-treated total RNA (2 μg of total RNA) using random hexamers. Quantification of firefly luciferase mRNA and mCherry mRNA (internal control) was performed on Applied Biosystems 7300 real-time PCR system using Power SYBR Green Master Mix (Applied Biosystems). Samples were run in triplicate, and the average cycle threshold (*C*T) was calculated. The average luciferase *C*T value for each sample was normalized to the corresponding average mCherry *C*T value to obtain a Δ*C*T value. The fold change in luciferase mRNA expression relative to reporter only samples was calculated using the comparative *C*T (ΔΔ*C*T) values. Primer sequences used for firefly luciferase were 5′-GCTATTCTGA TTACACCCGA GG-3′ and 5′-TCCTCTGACA CATAATTCGC C-3′ and for mCherry were 5′-CACTACGACG CTGAGGTCAA-3′ and 5′-GTAGTCCTCG TTGTGGGAGG-3′.

CRISPR/dCAS9-VP64 studies

HEK293T cells were transfected using Lipofectamine 3000 (Invitrogen) with 255 ng gRNA expression plasmid (63.75 ng of plasmid DNA encoding each of four gRNAs targeting *IL1RN* or the off-target control *HBG1*) and 245 ng of pcDNA3.1-CRY-dCas9-VP64. Primer sequences and standard curves were previously described (20). IL1RN gRNAs were CR1 (TGTACTCTCTGAGGTGCTC, at –29), CR2 (ACGCAGATAAGAACCAGTT, at –180), CR3 (CA TCAAGTCAGCCATCAGC, at –113), CR4 (GAGTCA CCCTCCTGGAAAC). HBG1 control gRNAs were CR1 (GCTAGGGATGAAGAATAAA, –26), CR2 (TTGACC AATAGCCTTGACA, –101), (TGCAAATATCTGTCTG AAA, –163), (AAATTAGCAGTATCCTCTT, –209). As a negative control cells were transfected with 500 ng of an empty pCMV plasmid. Cells were either illuminated with blue light using a custom-built 6 × 4 LED array (1 s pulses every 15 s, 450 nm, 16 mW/cm^2) starting 4 h after transfection or incubated in the dark for the entire experiment. Three days after transfection total mRNA was purified using Qiagen RNeasy spin prep columns. cDNA was synthesized using the SuperScript® VILO cDNA Synthesis Kit (Life Technologies). Relative levels of cDNA were detected using Quanta PerfeCta® SYBR® Green FastMix® (Quanta Biosciences) and CFX96 Real-Time PCR Detection System (Bio-Rad). Raw data was normalized to GAPDH levels and cells transfected with an empty plasmid control using the Δ*C*T method.

Immunoblotting

For total cell preps, cells were washed in 1× PBS, collected, and lysed in 2× Laemmli sample buffer with boiling. Proteins were separated by electrophoresis on an SDS-PAGE gel and transferred to nitrocellulose membranes, followed by probing with primary antibodies: GFP (G1544, Sigma-Aldrich, dilution 1:3750), beta-actin (sc-47778, Santa Cruz Biotechnology, dilution 1:1000), mCherry (PA5-34974, Thermo Scientific, dilution 1:1000), α-tubulin (926-42213, LI-COR, dilution 1:1000), or Gal4DBD (sc-577, Santa Cruz Biotechnology, dilution 1:1000). IRDye® secondary antibodies (dilution 1:15 000) and an Odyssey® FC Imager (LI-COR) were used to detect and visualize the target protein in the membrane.

Immunofluorescence staining

Cells grown on coverslips were washed with PBS then fixed with 4% paraformaldehyde in PBS for 15 min. Coverslips were washed with PBS and permeabilized/blocked in 5% Normal Goat Serum (Jackson ImmunoResearch Laboratories) and 0.1% Triton® X-100 (Amresco) in PBS for 1 h. Cells were incubated at room temperature for 2 h with anti-Gal4BD primary antibody (Santa Cruz Biotechnology, sc-577) in permeablization buffer. Cells were washed in PBS and incubated with AlexaFluor® 488 Goat anti-rabbit IgG (Invitrogen) for 1 h. Cells were washed in PBS and mounted on slides with FluoromountG® (SouthernBiotech).

Imaging

HEK293T cells were cultured in DMEM with 10% FBS, then seeded onto 35-mm glass bottom dishes or on coverslips in 12-well plates prior to transfection. Calcium phosphate or Lipofectamine 2000 (Life Technologies) was used for transfection, according to the manufacturer's protocol. For imaging of fixed cells, cells were washed in PBS, fixed in 4% paraformaldehyde, and mounted on glass slides using Fluoromount-G (Southern Biotech). For live cell imaging, cells were grown in glass bottom dishes, then media was exchanged for HBS with 1 mM $CaCl_2$ and samples were imaged at 33.5°C. Samples were protected from ambient light sources using a red safelight and by focusing in the presence of filtered light (572/28 bandpass filter, Chroma). Cell imaging was performed on either: (i) an Olympus

IX71 microscope equipped with a spinning disc scan head (Yokogawa Corporation of America) with a 60×/NA 1.4 objective. Excitation illumination was delivered from an AOTF controlled laser launch (Andor Technology) and images collected on a 1024 × 1024 pixel EM-CCD camera (iXon; Andor Technology) using Metamorph (Molecular Devices) software. (ii) A Ziess AxioObserver Z1 Inverted Spinning Disc Confocal Microscope with a 63×/NA 1.4 objective. Excitation illumination was delivered by a 3i Ablate!™ Model 3iL13 and image collected using a Yokogawa CSU-X1CU camera. Slidebook 6 was used for all collection of images on this system.

Spatial patterning studies were performed with HEK293T cells on 10 cm plates and were imaged with an UltraThin LED Illuminator (GelCompany, TBL-01) using an iImage GelDoc imaging stage with PureShot imaging software on an iPhone 6S platform.

Image analysis

After initial image collection, ImageJ 1.45s was used for all image analysis. For nuclear:cytoplasmic quantification, confocal image Z-stacks were first compiled into a maximal projection. Total fluorescence in either the nucleus or cytosol was calculated by manually selecting either the nucleus or cytosolic region of interest and quantifying average fluorescence and area within these compartment. A separate region of the image was used to calculate background, which was subtracted from the average fluorescence. Average fluorescence was multiplied by area and calculated for nuclear versus cytosolic regions, then these were divided to obtain a ratio of nuclear: cytosolic protein.

For zebrafish image quantification, we calculated the total fluorescence for each embryo (average fluorescence × area), after background subtraction. All embryos (including control uninjected embryos) showed significant autofluorescence, as indicated on graph. To control for variation in size between embryos in different groups, we normalized to a single, representative size, equal to the average. Nine embryo images were analyzed for light/dark samples, and seven for controls. Statistical significance for experiments comparing two populations was determined using a two-tailed unpaired Student's *t*-test.

Zebrafish studies

A UAS-GFP transgenic zebrafish line (Tg(5xUAS:EGFP)nkuasgfp1a) was used (21). This line was generated by the Kawakami laboratory (National Institute of Genetics, Japan) and was a kind gift from Maximiliano Suster (University of Bergen). The permits for the experiments were obtained from the Office of the Regional Government of Southern Finland in agreement with the ethical guidelines of the European convention.

Embryos were staged in hours post-fertilization (hpf). Developing embryos were injected at the one cell stage then incubated for 3 h at 28°C in room light to recover from injections. After 3 h (at 3 hpf) embryos were either placed under blue light (10 s pulse every 3 min, 5 mW/cm^2) or put in the dark. The light source was a custom LED array (470 nm). Light treatment was maintained for the duration of the experiment. At indicated times, embryos were fixed in 4% paraformaldehyde in PBS, then washed with PBS and dechorionated. Embryos were subsequently incubated with 50% glycerol for 1 h and transferred to 80% glycerol in PBS. Embryos were kept in 80% glycerol in PBS at 4°C, then placed on glass slides for imaging. Imaging was carried out using a Leica TCS SP2 AOBS Confocal microscope (Leica Microsystems, Mannheim, Germany). Stacks of images were taken at 1.1 μm intervals (z-axis) using an argon laser and compiled to maximum intensity projection images using Leica Confocal Software. For toxicity testing (Supplemental Table S1), embryos were injected with 20 pg CRY-GalVP16, treated with the same light/dark conditions as above, and assayed for viability at 27 hpf. Data is expressed as number of live embryos/number of embryos injected. Each group contained $n = 20$–43 embryos and each experiment was repeated three times.

RESULTS

Our previous approach to regulate transcription in yeast used a light-dependent interaction between CRY2 and its binding partner, CIB1, to reconstitute a split transcription activator binding domain and activation domain (14). While the method worked well in yeast with several different transcription factors (14–16), attempts to regulate transcription in mammalian cells using the same approach, with Gal4 DNA binding domain-CRY2 (GalBD-CRY2) and VP16 activation domain-CIB1 (VP16-CIB1) fusion proteins, showed no light dependence (Figure 1A).

To investigate why this approach was not immediately transferrable to mammalian cells, we examined localization of the GalBD-CRY2 fusion protein in light and dark. While cells incubated in dark showed strong nuclear localization of GalBD-CRY2, those incubated in light showed clearing of nuclear protein (Figure 1B). To functionally test whether nuclear clearing could affect activity, we fused CRY2 to either a Gal4BD-VP16AD synthetic transcription factor (22) (CRY-GalVP16) or a commonly used 'tTA' (Tet-OFF) transcriptional activator (1) (CRYΔNLS-mCh-tTA) and examined protein activity and localization. While CRY-GalVP16 and CRYΔNLS-mCh-tTA showed good activity in dark, function was significantly reduced after blue light illumination, inducing expression of a luciferase reporter to 3.6% of dark levels with CRY-GalVP16 (Figure 1C), and to 6.8% of dark levels with CRYΔNLS-mCh-tTA (Figure 1D). This functional loss was not due to a reduction in overall protein abundance: CRY-GalVP16 and CRYΔNLS-mCh-tTA showed no reduction in steady-state protein levels in light (Figure 1E). However, similar to observations with the GalBD-CRY2 fusion, both CRY-GalVP16 and CRYΔNLS-mCh-tTA showed substantially altered nuclear localization after light exposure (Figure 1F). In comparison, a CRY2-mCherry construct that did not contain a fused transcription factor showed only minimal protein redistribution with similar light treatment (Supplementary Figure S1).

We hypothesized that functional loss of activity and redistribution in light could occur through active processes of nuclear export, by blocking import of newly synthesized protein, or through a combination of these processes. Alternatively, protein could be degraded or sequestered

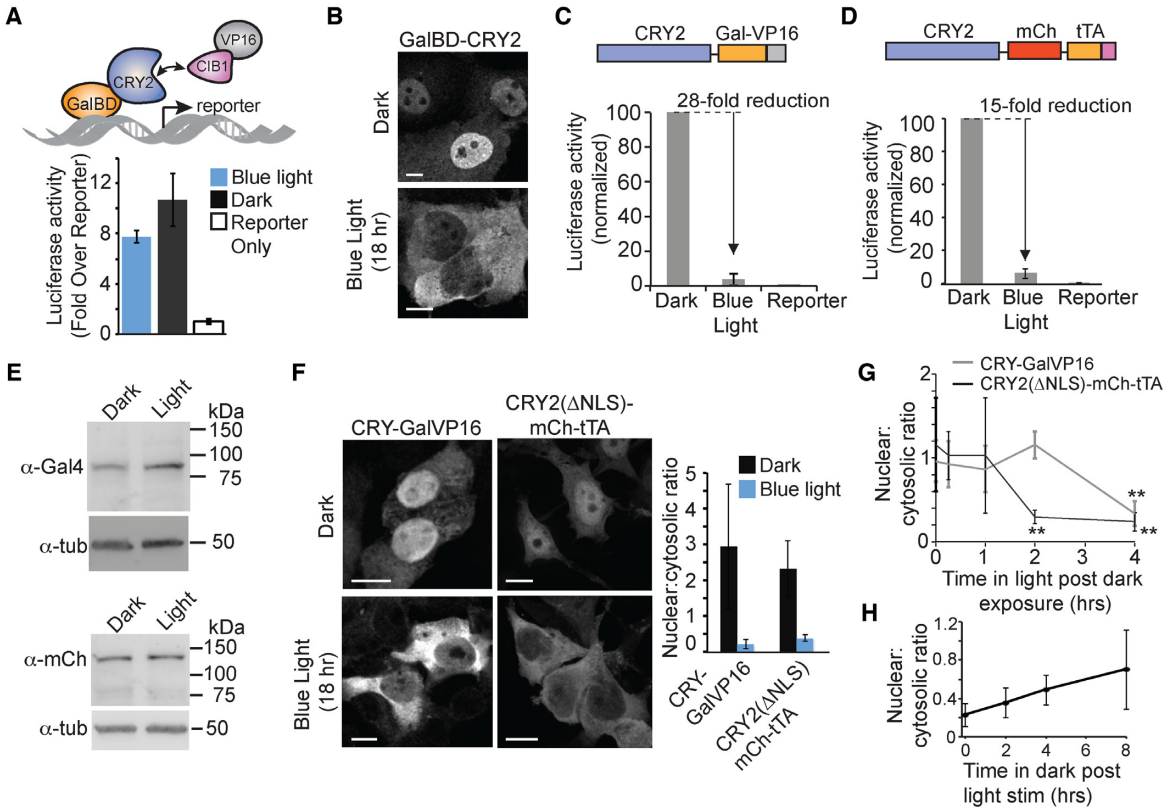

Figure 1. CRY2-fused transcription factors are cleared in the nucleus with light. (**A**) Schematic and luciferase activity of mammalian split transcriptional system using GalBD-CRY2 and VP16AD-CIB1. HEK293T cells were transfected with the AD and BD constructs and a *GalUAS*-luciferase reporter, then incubated in dark or exposed to light pulses for 18 h before assaying for luciferase activity. Fold increase in luciferase activity is shown compared to reporter only controls. Data represents average and error (s.d.) for three independent experiments. (**B**) Representative HEK293T cells expressing GalBD-CRY2 kept in dark or exposed to blue light pulses for 18 hrs., immunostained using an anti-Gal4BD antibody. Scale bar, 10 μm (**C** and **D**) Luciferase activity of HEK293 cells expressing CRY-GalVP16 and a *GalUAS*-luciferase reporter (C) or CRY2ΔNLS-mCh-tTA and a *7xtetO*-luciferase reporter (D) incubated 18 h in dark or with blue light pulses. Data represents average and error (s.d.) for three independent experiments. (**E**) Immunoblot of HEK293T cells expressing CRY-GalVP16 (top) or CRY2ΔNLS-mCh-tTA (bottom) and exposed to dark or light pulses for 18 h. Samples were also blotted with α-tubulin as a loading control. (**F**) Representative immunostaining (CRY-GalVP16, Gal4BD antibody) or fluorescence (CRY2(ΔNLS)-mCh-tTA) images showing localization of CRY2-fused proteins exposed to dark or light for 18 h. The ratio of nuclear:cytosolic protein from multiple cells is quantified in graph at right. Data represents average and error (s.d., $n = 10$). Scale bar, 10 μm. (**G**) Kinetics of nuclear clearing. Cells expressing CRY2 fusion constructs were incubated in dark for 16 h, then exposed to blue light pulses for indicated times before fixation. The ratio of nuclear:cytosolic protein from fixed cells was then quantified. Data represents average and error (s.d., $n = 4$). ***P*-value < .05. (**H**) Reversibility of phenotype. HEK293T cells expressing CRY2(ΔNLS)-mCh-tTA were treated with light for 18 h, then incubated in dark for indicated times before fixing and quantifying nuclear:cytoplasmic ratio as in (G). Data represents average and error (s.d., $n = 8$).

in inactive complexes. We carried out further experiments to examine the timecourse of the nuclear clearing phenotype, to distinguish between very rapid nuclear clearing in light, suggesting a role of nuclear export pathways, versus a slower phenotype, suggesting a slower process such as protein degradation or sequestration, or even passive dilution of nuclear protein as cells divide over time. We examined the change in nuclear abundance in light versus dark of the two constructs, tracking the fluorescent reporter-tagged CRYΔNLS-mCh-tTA protein, or by immunostaining CRY-GalVP16 protein using an anti-Gal4BD antibody. In both cases, nuclear clearing occurred over several hours (Figure 1G). As HEK293T cells have a doubling time of ∼20 h, the nuclear redistribution occurs more quickly than would be seen with passive dilution. On the other hand, light-triggered nuclear export—in which light results in binding to a NES-containing protein or exposure of a cryptic NES—would be expected to result in much faster protein depletion. The several hour timeframe for clearing suggests a slower process, for example related to protein degradation, protein sequestration, or nuclear quality control.

We next examined recovery of nuclear protein, upon moving from light to dark. Restoration of cleared protein, upon switching cells from light illumination to dark, was even slower and more heterogeneous. While the majority of cells showed partial recovery of nuclear protein after four hours and full recovery after 8 h (Figure 1H), some cells showed minimal nuclear protein even after eight hours. The slow timecourse of recovery of nuclear protein is consistent with new protein synthesis or slow protein redistribution from the cytosol.

In previous studies, some CRY2-tagged target proteins have been observed to cluster with light application, in particular when expressed in concentrated intracellular compartments (23–28). To examine potential clustering of CRY2-transcription factor fusion proteins we imaged cells

expressing CRYΔNLS-mCh-tTA. With light stimulation, nuclear CRY2ΔNLS-mCh-tTA rapidly redistributed into clusters, which coalesced into larger puncta over tens of minutes (Figure 2A). Prior studies of CRY2 demonstrated enhancement of light-dependent clustering upon fusion of CRY2 to multivalent proteins (26–28). Since the transcription factors we fused to CRY2 are known to dimerize, we investigated whether the presence of a dimerization domain could contribute to the nuclear clearing and loss-of-function phenotype. We replaced residues 1–147 of the Gal4 DNA binding domain of GalVP16 with a truncated version (GalΔDD) lacking residues 66–95, previously shown to be important for dimerization (29) (Figure 2B). This construct, GalΔDD-VP16, retains only a minimal dimerization motif (30) and cannot stimulate transcription on its own (Supplementary Figure S2), consistent with the critical importance of the dimerization domain for DNA binding. Fusion of GalΔDD-VP16 to CRY2 restores activity to a large extent (Supplementary Figure S2), likely because CRY2, which oligomerizes in light but also shows some degree of self-association in dark (18), substitutes for the missing dimerization domain. In contrast to CRY-GalVP16, which shows good activity in dark but diminished function in light, CRY-GalΔDD-VP16 showed no reduction in activity with light but instead a slight increase (Figure 2C), possibly due to oligomerization of DNA-bound CRY-GalΔDD-VP16 with unbound CRY-GalΔDD-VP16 protein. In concert with the functional results, CRY-GalΔDD-VP16 shows no light dependent change in localization even with extended light treatment (Figure 2D).

To further investigate the dependence of the loss-of-function phenotype on the presence of a dimerization domain, we tested whether adding back a different dimerization domain to CRY-GalΔDD-VP16 could recover light dependence. Insertion of dsRed, a 28 kDa tetramerizing protein, between CRY2 and GalΔDD-VP16s (Figure 2E) restored light-dependent nuclear loss (Figure 2F) and light-dependent loss of transcriptional activity (Figure 2G). In contrast, a construct containing mCherry, a 29 kDa monomeric protein, at the same site showed similar behavior as CRY-GalΔDD-VP16, with no light-dependent loss of activity (Figure 2H). These results suggest that the presence of a dimerization motif is important for conferring light/dark functional and localization differences.

An optimized light-activated system for transcriptional control

Our results showing sustained nuclear localization with light-treated CRY-GalΔDD-VP16 led us to revisit the split transcription system described in Figure 1A, substituting the full Gal4 DNA binding domain (residues 1–147) with a shorter version of the Gal4ΔDD (Gal4 residues 1–65) (Figure 3A). While the original GalBD-CRY construct had shown substantial nuclear redistribution with light (Figure 1B), CRY-Gal(1–65) showed minimal localization changes (Figure 3A). When coexpressed with VP16-CIB1, CRY-Gal(1–65) showed greatly enhanced light-stimulated activity with low background activity in dark (Figure 3B). To optimize this system for regulation of transcription in mammalian cells, we tested alternate CIB-AD constructs (Figure 3c). While use of VP16-CIB1 showed 15.1-fold activation over dark levels, a CIB1-VP16-CIB1 construct containing an additional copy of CIB1 at the N-terminus, which showed improved function within a CRY2-CIB dimerized split CRISPR/dCas9 system (31), showed only a modest 2-fold increase in dynamic range (27.6-fold activation over dark levels). A construct containing a N-terminal CIB1 fusion (CIB1-VP16) achieved higher levels of light-dependent activity, but also showed higher dark background. Replacement of the VP16 activation domain with a stronger VP64 domain (CIB1-VP64) provided the highest level of activation, with only a small increase in dark background over VP16-CIB1 (101.8-fold activation over dark levels) (Figure 3C). A *GalUAS*-GFP reporter used with CRY-Gal(1–65) and VP16-CIB1 also showed low or no background in dark, and good induction of reporter expression in light (Figure 3D).

The use of light for transcriptional regulation provides the important advantages of spatiotemporal and dose-dependent control. We carried out additional experiments to evaluate spatial, dose-dependent, and temporal regulation of the optimized split system. To monitor potential for spatial control, we delivered patterned light to HEK293T cell monolayers expressing CRY-Gal(1–65), CIB1-VP64, and a *GalUAS*-GFP reporter, which induced reporter expression specifically in areas exposed to light (Figure 3E). Reporter expression was sensitive to light levels and highly tunable by varying light intensity used in experiments (Figure 3F). To monitor reversibility of the system, we incubated cells expressing CRY-Gal(1–65), CIB1-VP64, and a GalUAS-luciferase reporter in light for 12 h to initially induce reporter activity, then monitored reporter responses over the next 12 h in response to four different light illumination conditions (dark/dark, dark/light, light/dark, light/light), with each light treatment lasting 6 h (Supplementary Figure S3). Cells incubated in 12 additional hours of light showed the highest levels of luciferase activity, compared with cells incubated in 6 h light then 6 h dark, or those incubated in 6 h dark then light. Cells incubated in dark for 12 h showed minimal increase in luciferase activity over the duration.

Light-disrupted system for transcriptional control

In addition to generating a split transcriptional system activated by blue light, we considered that light-dependent nuclear clearing, while counteracting our ability to stimulate transcription with light, could be harnessed as a means to negatively regulate transcription or other nuclear protein activity upon blue light exposure. To optimize the CRY-GalVP16 system, we used a longer version of VP16 and removed the mCherry-IRES element present in the original construct. In dark, this construct, CRY-GalVP16l, activated a *GalUAS*-luciferase reporter ∼2-fold better than intact Gal4 (Figure 4A). Application of blue light for 24 h resulted in a 37-fold reduction in luciferase expression (to 2.7 ± 0.6% of dark levels). *GalUAS*-luciferase mRNA was also reduced in light compared with dark (Figure 4B). Disruption of reporter expression with light was comparable to that obtained using cycloheximide to block translation (Supplementary Figure S4). Reporter expression could be

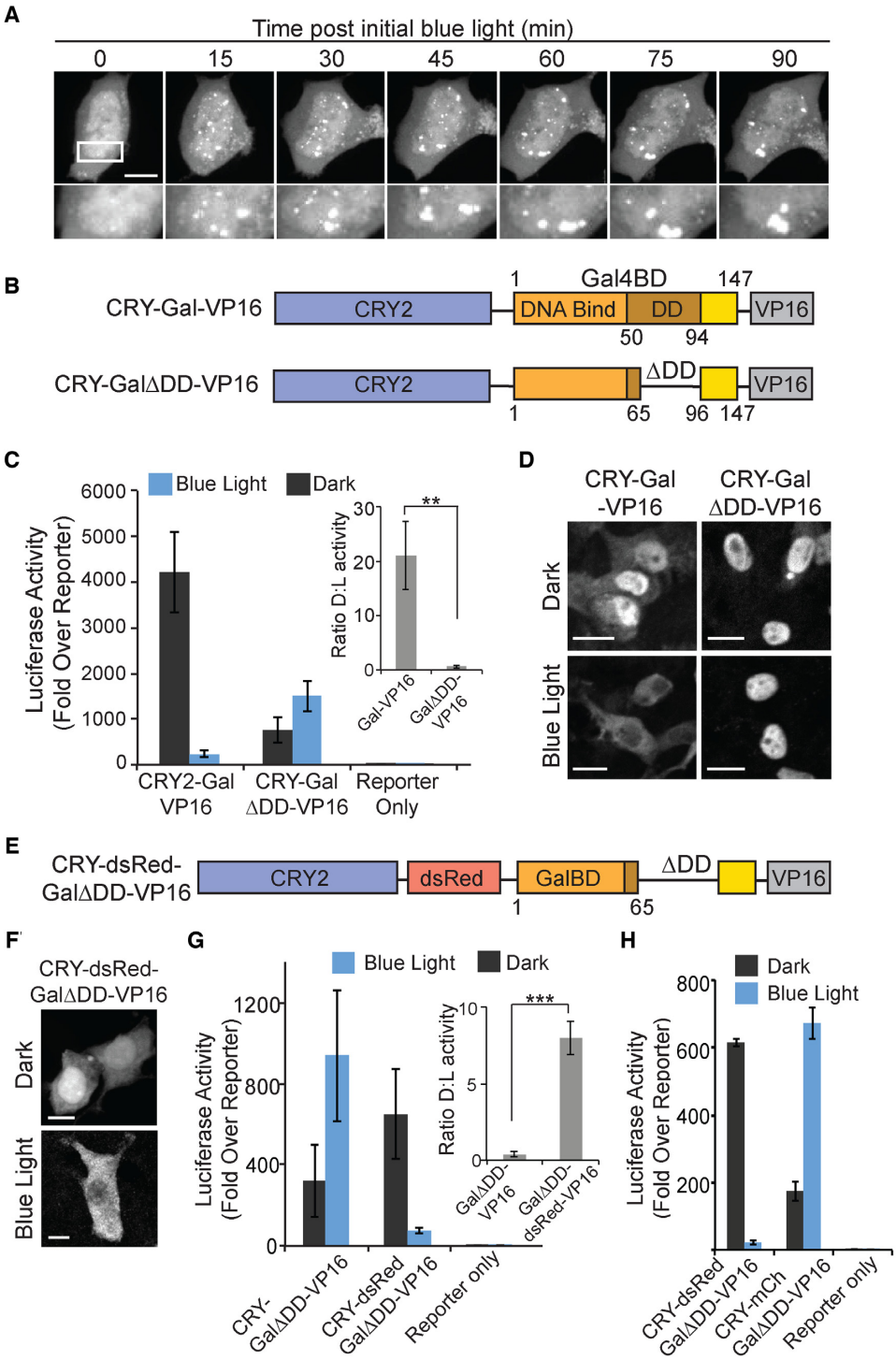

Figure 2. A CRY2-fused dimerization domain is required for light-dependent nuclear clearing and functional loss of activity. (**A**) Live cell imaging showing formation of CRY2(ΔNLS)-mCh-tTA clusters in the nucleus upon initial light exposure, which coalesce into larger puncta over the 90 min timecourse. Scale bar, 10 μm. (**B**) Schematic showing constructs used in (C) and (D). CRY-GalΔDD-VP16 contains Gal4BD residues 1–147 but is missing residues 66–95, which are important for dimerization. (**C**) Luciferase activity of cells expressing indicated constructs exposed to 18 h dark or blue light pulses. Data represents average and error (s.e.m.) from four independent experiments. Inset shows the ratio of activity in dark to activity in light. ***P*-value < .05. (**D**) Localization of protein fusions in HEK293T cells, assayed by immunohistochemistry using an anti-Gal4BD antibody. Cells were treated as in (C). (**E–G**) Addition of a tetramerizing dsRed domain restores light response to CRY-GalΔDD-VP16. (E) Schematic of construct used in (F) and (G). (F) Representative HEK293T cells expressing CRY-dsRed-GalΔDD-VP16, exposed to 18 h dark or blue light pulses, and assayed for localization as in (C). (G) Luciferase activity of cells expressing CRY-GalΔDD-VP16 alone or with an added back multivalent domain (CRY-dsRed-GalΔDD-VP16) assayed as in (C). Data represents average and error (s.e.m.) for three independent experiments. Inset shows the ratio of activity in dark to activity in light. ****P*-value < .005. (**H**) Comparison of effect of adding back a tetramerizing dsRed domain versus a monomeric mCherry domain to CRY-GalΔDD-VP16. Luciferase assay was carried out as in (C). Data represents average and error (s.d., $n = 3$) from one experiment, and experiments were repeated two times with similar results.

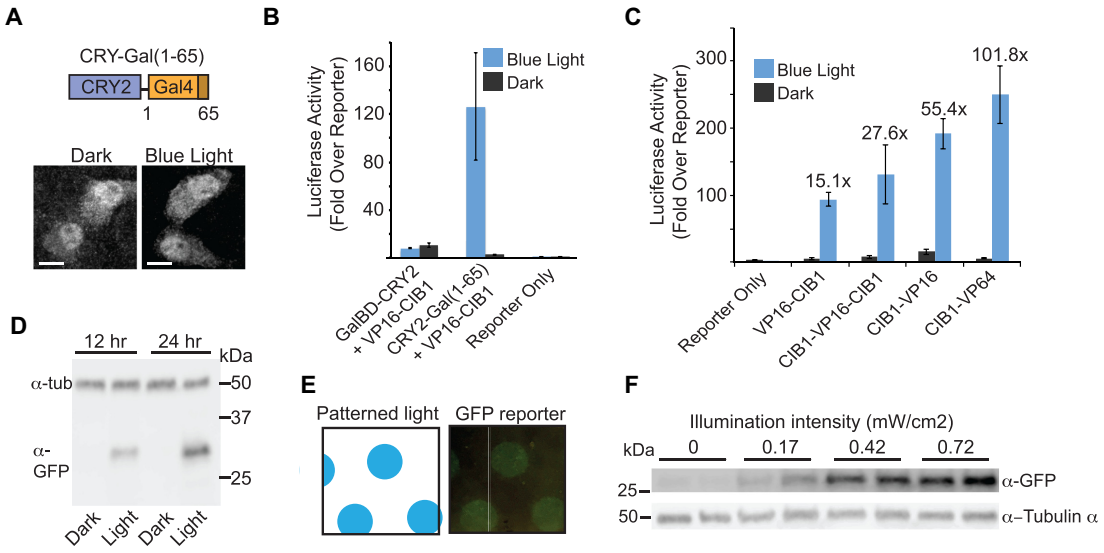

Figure 3. Optimization of split CRY2/CIB1 transcriptional system. (**A**) Schematic and immunostaining of new CRY2-BD construct (CRY-Gal(1–65)) assayed in split transcriptional system. HEK293T cells expressing CRY2-Gal(1–65) were kept in dark or exposed to blue light pulses for 18 h, then assayed for immunohistochemistry using an anti-Gal4BD antibody. (**B**) Luciferase activity of HEK293T cells expressing indicated constructs and a GalUAS-luciferase reporter and exposed to dark or blue light pulses as in (A) for 18 h. Data represents average and error (s.d., $n = 3$). Experiments were repeated two times with similar results. (**C**) Comparison of activation domain fusions. HEK293T cells were transiently transfected with CRY2-Gal(1–65) and indicated AD-fusion constructs, along with a GalUAS-luciferase reporter and tested for activity as in (B). Data represents average and error (s.d., $n = 3$). Experiments were repeated three times with similar results. (D) Immunoblot of HEK293T cells expressing a *GalUAS*-GFP-HA reporter with CRY2-Gal(1–65) and CIB1-VP64 incubated in dark or blue light for 18 h. (**E**) Spatial regulation. HEK293T cells expressing CRY-Gal(1–65), VP64-CIB1, and a *GalUAS*-GFP reporter were exposed to 18 h patterned blue light, followed by imaging of GFP reporter expression. Scale bar, 1 cm. (**F**) Dose-dependent regulation. HEK293T cells expressing constructs as in (E) were illuminated with varying light intensities for 18 h, followed by immunoblotting using an anti-GFP antibody or anti-tubulin control.

spatially controlled by delivery of patterned light (Figure 4C) and could be temporally and reversibly regulated by altering light conditions (Supplementary Figure S5).

To optimize the tTA-regulated system, we removed the mCherry tag from CRYΔNLS-mCh-tTA to generate CRY-tTA, which induced robust transcription of a *tetO*-luciferase reporter in dark but showed significantly reduced luciferase expression, to 2.3% of dark levels, with blue light exposure (Figure 4D). Loss of transcriptional activity with light was substantial but not as effective as use of doxycycline, which disrupts binding of the Tet repressor to DNA (4-fold over background with CRY-tTA + light, compared with 2-fold over background with tTA + doxycycline). Loss of luciferase reporter expression with light with CRY-tTA also correlated with a reduction in mRNA levels (8-fold reduction with light) (Figure 4E). A version of CRY-tTA (CRY2olig-tTA) in which CRY2 was substituted with CRY2olig(FL), a E490G version of CRY2 showing enhanced clustering properties (26), also showed functional loss in light (to 3.9% of dark levels), but no significant enhancement of this phenotype due to enhanced clustering (Supplementary Figure S6).

We examined whether the basic approach used with tTA and GalVP16 could be extended to regulate transcription at endogenous genomic loci with dCas9 (a D10A, H840A catalytically inactive Cas9 (20,32–34). We fused CRY2 to a fusion of dCas9 and VP64, generating CRY2-dCas9-VP64. We coexpressed this construct along with a gRNA targeting the human IL1RN promoter in HEK293T cells. Cells incubated in dark showed strong induction of IL1RN mRNA levels that was reduced ∼4-fold with light exposure (Figure 4F), indicating this approach can also regulate transcription at endogenous genomic sites using CRISPR/Cas9 technology.

We tested if our system for light-mediated disruption of transcription could function *in vivo*, using zebrafish (*Danio rerio*) as a vertebrate model system. We monitored the ability of CRY-GalVP16l to regulate gene expression in *GalUAS*-GFP transgenic zebrafish embryos, which express GFP under control of a 5x*GalUAS* promoter. Embryos were microinjected at the one-cell stage with the CRY-GalVP16l plasmid (20 pg DNA/embryo) then exposed to light or placed in the dark. Zebrafish grown in the light showed a significant reduction of GFP expression compared with dark-grown fish, which was observable at 12 and 27 h post-fertilization (hpf) (Figure 4G and H). The dosage used (20 pg) showed only minimal toxicity (Supplementary Table S1), which may be due to the presence of the full length VP16 activation domain (35). Together, our data indicates the system is functional *in vivo* in vertebrates.

While the above light-disrupted transcriptional approaches showed significant light/dark differences, they were suboptimal for two reasons. First, we were unable to find conditions such that we could completely block transcription with light: some transcript always remained even with light application. Second, even if the system could be optimized to completely block transcription, existing protein can last for hours to days within cells, limiting the utility of this approach. To overcome these limitations, we tested whether we could combine the light-disrupted transcrip-

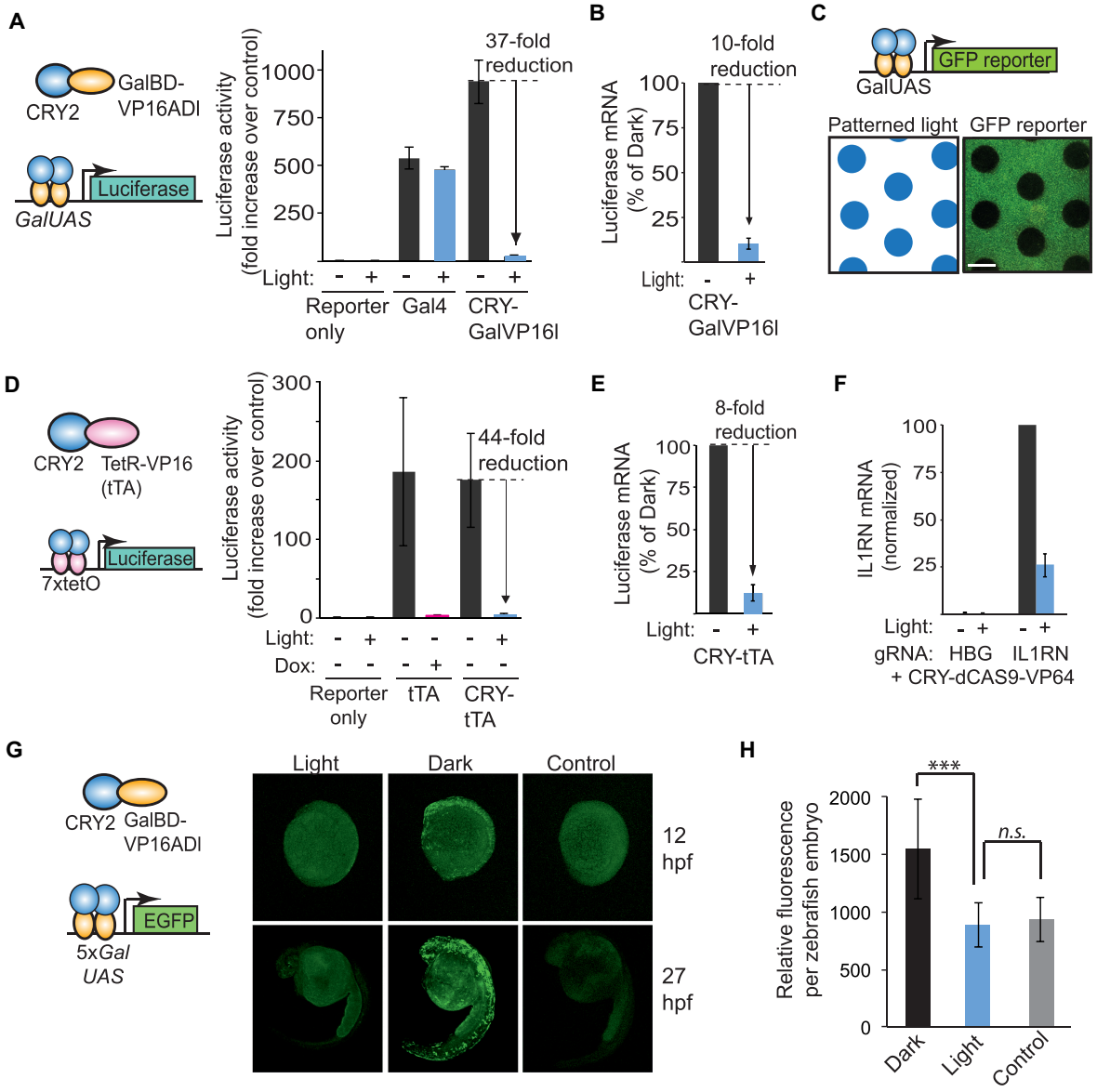

Figure 4. Light-mediated disruption of transcription. (**A**) Schematic and luciferase activity of optimized light disrupted system. HEK293T cells were transiently transfected with a *GalUAS*-luciferase reporter and control DNA (reporter only), CRY-GalVP16I, or intact Gal4, grown for 24 h in dark or pulsed blue light, then assayed for luciferase activity. Fold increase in luciferase activity is shown compared to reporter controls. Data represents average and error (s.d., $n = 3$). (**B**) Quantitative RT-PCR showing luciferase mRNA levels in cells transfected as in (A) and harvested after 22 h. Shown is the average and range from two independent experiments (experiments were repeated two additional times with similar results). (**C**) Spatial regulation. HEK293T cells transiently transfected with CRY-GalVP16I and a *GalUAS*-GFP reporter were exposed to patterned blue light for 18 h before imaging. Scale bar, 1 cm. (**D**) Schematic and luciferase activity of HEK293T cells transiently transfected with a *7xtetO*-luciferase reporter and either CRY-tTA, tTA or control DNA (reporter only). Luciferase activity was measured after 24 h. incubation in dark or blue light pulses. Doxycycline samples included 0.5 μM doxycycline. Data represents average and error (s.d.) from three independent experiments. (**E**) Quantitative RT-PCR showing the levels of luciferase mRNA in HEK293T cells transfected as in (D) and harvested after 22 h. Data represents average and standard deviation from three independent assays. (**F**) Light regulation of endogenous *IL1RN* transcription using a CRISPR/dCAS9-based approach. HEK293T cells were transfected with CRY-dCas9-VP64 and *IL1RN* or *HBG1*-targeted gRNAs and exposed to light (1 s pulses every 15 s) or dark for 3 days. Data represents average and range for two independent experiments (three replicates each). (**G**) *In vivo* testing of CRY-GalVP16I in *GalUAS*-GFP reporter zebrafish embryos. Embryos were injected with 20 pg CRY-GalVP16I DNA at the one-cell stage and then incubated (after a 3 h recovery period) in the dark or light (10 s pulse every 3 min, 470 nm, 5 mW/cm^2). GFP images of representative embryos were acquired at 12 and 27 hpf. Controls show images of non-injected embryos at 12 and 27 hpf. (**H**) Quantification of zebrafish embryo fluorescence. Embryos treated as described in (G) were imaged then quantified for total fluorescence ($n = 7$–9 embryos each condition). Control embryos showed significant autofluorescence as indicated. ***P-value < .005. n.s., not significant.

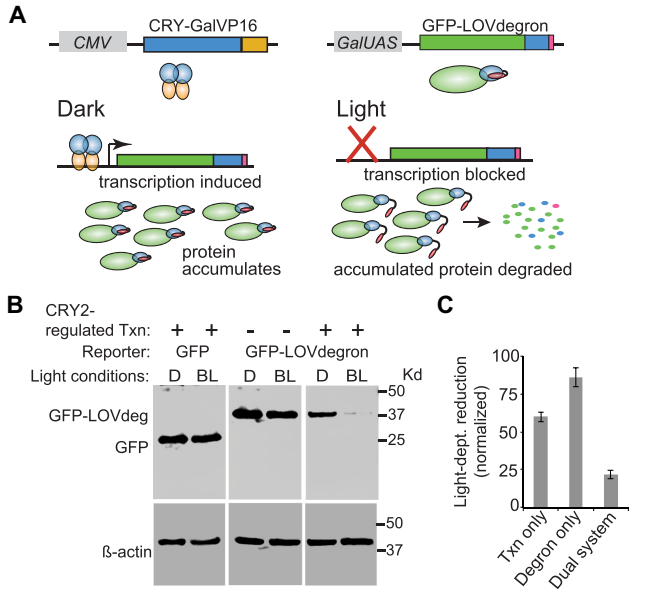

Figure 5. A dual optogenetic system for depleting protein with light. (**A**) Schematic demonstrating a dual optogenetic system allowing light inhibition of transcription combined with stimulation of protein degradation. (**B**) Immunoblot of HEK293T cells expressing CRY-GalVP16 and a *GalUAS*-GFP-LOVdeg reporter in light or dark. Cells were incubated for 17.5 h in dark to induce protein, then kept in dark or exposed to blue light pulses for an additional 3.5 h (2 s pulse every 45 s). Control samples with cells expressing single optogenetic systems alone (expressing a constitutive *CMV*-GFP-LOVdeg reporter, or expressing CRY-GalVP16 and pGL2-*GalUAS*-GFP-HA), retained higher levels of GFP after light illumination compared with the dual system. (**C**) Quantification of reduction in protein levels induced with light. Graph shows protein light levels expressed as a percent of dark levels. Data shows average and range from two independent experiments.

tional system with a system allowing light-dependent degradation of existing protein. Previously, a light-inducible degron based on the *Avena sativa* phototropin1 LOV2 domain was developed that allows stimulation of protein degradation with light upon attachment of a small tag at the C-terminus of a protein of interest (36). As both CRY2 and the LOV-based degron are activated by blue light, we reasoned that we could combine these approaches to generate a dual optogenetic system, allowing a single light stimulus to block new mRNA transcription, and in turn deplete existing protein fused to the LOV-degron (Figure 5A). We fused EGFP to a C-terminal LOV-degron (36), which was placed under GalUAS transcriptional control (*GalUAS*-GFP-LOVdeg). Cells were transiently transfected with CRY-GalVP16l and *GalUAS*-GFP-LOVdeg, incubated in the dark for 17.5 h to induce EGFP expression, then incubated in the dark or light for an additional 3.5 h. Cells incubated in light using the dual system showed a significant reduction in EGFP reporter expression compared to samples incubated in the dark (Figure 5B and C). Indeed, cells expressing the dual system (Figure 5B, right panel) showed much lower levels of GFP reporter compared with those using either system on its own (Figure 5B, left and middle panels).

DISCUSSION

Here we report that certain CRY2-fused transcription factors undergo substantial nuclear protein clearing with light, resulting in light-dependent loss of protein function. Nuclear clearing is dependent on the presence of a dimerization motif in the CRY2-attached protein: removal of this domain eliminates light-dependent nuclear redistribution, while adding back an orthogonal dimerization motif restores light dependence. Upon light stimulation, we observe the sequestration of CRY2-fused transcription factors into nuclear clusters. Sequestered protein is cleared within the nucleus over a time frame of 2–4 h, a process faster than passive dilution (due to cell growth) but slower than active nuclear export. While our imaging studies indicate clearing of nuclear protein over this time frame, we note that our approaches do not distinguish between loss of protein within the nucleus, versus clearing and redistribution of the protein to the nuclear periphery, resulting in functional loss of activity. In addition to nuclear clearing, we observe accumulation of CRY2-fused protein in the cytosol with light. We hypothesize that light-induced CRY2 cluster formation also blocks or slows nuclear import of cytosolic and newly synthesized protein, leading to accumulation of protein in the cytosol.

Our findings showing nuclear phenotypes dependent on CRY2 fusion proteins have impact for users of CRY2/CIB1 technologies for genomic control. Many groups have used CRY2/CIB1 for control of nuclear proteins such as CRISPR/dCas9, Cre DNA recombinase, transcription factors, or other enzymes (8,17,18,31,37). In cases in which CRY2 has been fused to a transcription factor DNA binding domain, light-dependent regulation was unexpectedly poor (7,8,17), likely due to the nuclear localization changes described here. Understanding how nuclear CRY2 fusion proteins behave will provide insight into better strategies for controlling nuclear protein activity that either circumvent or take advantage of nuclear clearing phenotypes.

We applied the knowledge gained in these studies to develop two methods to regulate transcription in the nucleus with light using CRY2. We optimized a light-activated split Gal4-VP16 transcriptional system brought together by the CRY2–CIB1 interaction, replacing a CRY–GalBD fusion that showed loss of nuclear localization with light with a version in which we deleted the Gal4BD dimerization domain. This fusion protein retained nuclear localization with light, and resulted in robust stimulation of transcription with light when used in conjunction with a CIB1-AD fusion protein. As a second approach to regulate transcription with light, we developed a generalizable single-construct system using CRY2 for light-dependent inhibition of transcription factor activity. As evidence of the generality of this system, we demonstrate light-regulated control of several transcriptional activators, including the commonly used tTA (tet-OFF) and Gal4-VP16 systems, as well as emerging CRISPR/Cas9 systems allowing regulation at endogenous loci. To achieve tighter control of protein levels, we combined this system with a light-regulated degron for dual optogenetic control, resulting in improvements over each system used independently.

A variety of light-regulated transcriptional systems for eukaryotes have been developed thus far, which have been used to regulate transcription in organisms including yeast, fly, zebrafish, and mouse (4–12,14–17,38,39). We feel the two approaches described here will complement and extend these existing methods. With light-inducible transcription, existing systems show various limitations, including moderate levels of background in dark depending on expression system used (9,10), a requirement for exogenous chromophore (4,5,38,39), limited reversibility (11,12), limited ability for local photoactivation (5,6), or a requirement for specific promotor elements (9). The CRY2/CIB1 split approach described here requires no exogenous chromophores or added factors, can be locally activated using readily available blue light sources, and can be utilized with commonly used GalUAS-based promoters. In particular, our initial tests of this light-activated system show extremely low background levels of transcription in dark, a critical parameter for achieving tight control of expression levels. While this system has been developed for use with *GalUAS* promoter elements, in further work other transcription factors, including tTA, can likely be implemented, allowing regulation of transcription from widely-used *tetO*-responsive promoters. Other improvements can include optimization of GalUAS binding sites on promoter elements, which can modulate light/dark dynamic range of reporter expression (11,39), and engineering the dimerization-deleted Gal4BD (Gal4 1–65) to achieve higher levels of light-induced activity.

While several alternate systems exist for inducing transcription with light, very few have been developed allowing reduction of transcription with light. One approach in zebrafish used addition of CRY2 to repress CIB1-mediated transcription, however this strategy required an uncommonly-used G-box promoter element (induced by CIB1), showed only modest light regulation, and needed two separate components (7). Our approach described here can be used with any number of transcription factors, and shows robust light-dependent regulation. A disadvantage of our method is that while there is a substantial reduction in transcriptional response in light, significant background activity remains, depending on initial expression level of the construct. However, by combining this approach with other regulatory approaches, as we demonstrate in Figure 5 combining the light-disrupted transcriptional system with a light-induced degron for dual light control of mRNA and protein levels, we can achieve much tighter control of expression. As our general approach requires only a single fusion construct, no added chemical cofactors, and can be easily packaged in viral vectors, we anticipate it will be useful for a variety of studies *in vivo*. We anticipate that a similar strategy could be used to regulate not only transcription factors, but also many other nuclear-specific enzymes and signaling effectors.

SUPPLEMENTARY DATA

Supplementary Data are available at NAR Online.

ACKNOWLEDGEMENTS

We thank the following scientists for providing constructs (distributed through Addgene): Thomas Wandless (pBMNHAYFP-LOV24, Addgene 49570), Liqun Luo (pCMV-Gal4, Addgene 24345; pBT224_pCA-tTA2, Addgene 36430), Martin Walsh (pGL2-*GAL4UAS*-Luc, Addgene 33020). We also thank James Hagman (National Jewish Medical Research Center) for providing GFP-Id1NES and Maximiliano Suster (University of Bergen) for providing transgenic UAS-GFP zebrafish. Light box construction was provided by the Optogenetics and Neural Engineering Core at the University of Colorado Anschutz Medical Campus, funded in part by the NIH (award number P30NS048154).

FUNDING

National Institutes of Health [GM100225 to C.L.T., DA036865 to C.A.G.]; National Science Foundation [CBET-1151035 to C.A.G.]; Academy of Finland [260030 to J.R.]. Funding for open access charge: Department funds.
Conflict of interest statement. None declared.

REFERENCES

1. Gossen,M. and Bujard,H. (1992) Tight control of gene expression in mammalian cells by tetracycline-responsive promoters. *Proc. Natl. Acad. Sci. U.S.A.*, **89**, 5547–5551.
2. Gossen,M., Freundlieb,S., Bender,G., Muller,G., Hillen,W. and Bujard,H. (1995) Transcriptional activation by tetracyclines in mammalian cells. *Science* **268**, 1766–1769.
3. Rennel,E. and Gerwins,P. (2002) How to make tetracycline-regulated transgene expression go on and off. *Anal. Biochem.*, **309**, 79–84.
4. Shimizu-Sato,S., Huq,E., Tepperman,J.M. and Quail,P.H. (2002) A light-switchable gene promoter system. *Nat. Biotechnol.*, **20**, 1041–1044.
5. Müller,K., Engesser,R., Schulz,S., Steinberg,T., Tomakidi,P., Weber,C.C., Ulm,R., Timmer,J., Zurbriggen,M.D. and Weber,W. (2013) Multi-chromatic control of mammalian gene expression and signaling. *Nucleic Acids Res.*, **41**, e124.
6. Crefcoeur,R.P., Yin,R., Ulm,R. and Halazonetis,T.D. (2013) Ultraviolet-B-mediated induction of protein-protein interactions in mammalian cells. *Nat. Commun.*, **4**, 1779.
7. Liu,H., Gomez,G., Lin,S.S. and Lin,C. (2012) Optogenetic control of transcription in zebrafish. *PLoS One*, **7**, e50738.
8. Konermann,S., Brigham,M.D., Trevino,A., Hsu,P.D., Heidenreich,M., Cong,L., Platt,R.J., Scott,D.A., Church,G.M. and Zhang,F. (2013) Optical control of mammalian endogenous transcription and epigenetic states. *Nature*, **500**, 472–476.
9. Motta-Mena,L.B., Reade,A., Mallory,M.J., Glantz,S., Weiner,O.D., Lynch,K.W. and Gardner,K.H. (2014) An optogenetic gene expression system with rapid activation and deactivation kinetics. *Nat. Chem. Biol.*, **10**, 196–202.
10. Wang,X., Chen,X. and Yang,Y. (2012) Spatiotemporal control of gene expression by a light-switchable transgene system. *Nat. Methods*, **9**, 266–269.
11. Polstein,L.R. and Gersbach,C.A. (2012) Light-inducible spatiotemporal control of gene activation by customizable zinc finger transcription factors. *J. Am. Chem. Soc.*, **134**, 16480–16483.
12. Yazawa,M., Sadaghiani,A.M., Hsueh,B. and Dolmetsch,R.E. (2009) Induction of protein-protein interactions in live cells using light. *Nat. Biotechnol.*, **27**, 941–945.
13. Liu,H., Yu,X., Li,K., Klejnot,J., Yang,H., Lisiero,D. and Lin,C. (2008) Photoexcited CRY2 interacts with CIB1 to regulate transcription and floral initiation in Arabidopsis. *Science* **322**, 1535–1539.
14. Kennedy,M.J., Hughes,R.M., Peteya,L.A., Schwartz,J.W., Ehlers,M.D. and Tucker,C.L. (2010) Rapid blue-light-mediated

induction of protein interactions in living cells. *Nat. Methods*, **7**, 973–975.
15. Hughes,R.M., Bolger,S., Tapadia,H. and Tucker,C.L. (2012) Light-mediated control of DNA transcription in yeast. *Methods*, **58**, 385–391.
16. Pathak,G.P., Strickland,D., Vrana,J.D. and Tucker,C.L. (2014) Benchmarking of optical dimerizer systems. *ACS Synth. Biol.*, **3**, 832–838.
17. Chan,Y.-B., Alekseyenko,O.V. and Kravitz,E.A. (2015) Optogenetic control of gene expression in Drosophila. *PLoS One*, **10**, e0138181.
18. Taslimi,A., Zoltowski,B., Miranda,J.G., Pathak,G.P., Hughes,R.M. and Tucker,C.L. (2016) Optimized second-generation CRY2-CIB dimerizers and photoactivatable Cre recombinase. *Nat. Chem. Biol.*, **12**, 425–430.
19. Gerhardt,K.P., Olson,E.J., Castillo-Hair,S.M., Hartsough,L.A., Landry,B.P., Ekness,F., Yokoo,R., Gomez,E.J., Ramakrishnan,P., Suh,J. *et al.* (2016) An open-hardware platform for optogenetics and photobiology. *Sci. Rep.*, **6**, 35363.
20. Perez-Pinera,P., Kocak,D.D., Vockley,C.M., Adler,A.F., Kabadi,A.M., Polstein,L.R., Thakore,P.I., Glass,K.A., Ousterout,D.G., Leong,K.W. *et al.* (2013) RNA-guided gene activation by CRISPR-Cas9-based transcription factors. *Nat. Methods*, **10**, 973–976.
21. Asakawa,K., Suster,M.L., Mizusawa,K., Nagayoshi,S., Kotani,T., Urasaki,A., Kishimoto,Y., Hibi,M. and Kawakami,K. (2008) Genetic dissection of neural circuits by Tol2 transposon-mediated Gal4 gene and enhancer trapping in zebrafish. *Proc. Natl. Acad. Sci. U.S.A.*, **105**, 1255–1260.
22. Sadowski,I., Ma,J., Triezenberg,S. and Ptashne,M. (1988) GAL4-VP16 is an unusually potent transcriptional activator. *Nature*, **335**, 563–564.
23. Mas,P., Devlin,P.F., Panda,S. and Kay,S.A. (2000) Functional interaction of phytochrome B and cryptochrome 2. *Nature*, **408**, 207–211.
24. Yu,X., Sayegh,R., Maymon,M., Warpeha,K., Klejnot,J., Yang,H., Huang,J., Lee,J., Kaufman,L. and Lin,C. (2009) Formation of nuclear bodies of Arabidopsis CRY2 in response to blue light Is associated with Its blue light–dependent degradation. *Plant Cell Online*, **21**, 118–130.
25. Ozkan-Dagliyan,I., Chiou,Y.-Y., Ye,R., Hassan,B.H., Ozturk,N. and Sancar,A. (2013) Formation of Arabidopsis Cryptochrome 2 photobodies in mammalian nuclei: application as an optogenetic DNA damage checkpoint switch. *J. Biol. Chem.*, **288**, 23244–23251.
26. Taslimi,A., Vrana,J.D., Chen,D., Borinskaya,S., Mayer,B.J., Kennedy,M.J. and Tucker,C.L. (2014) An optimized optogenetic clustering tool for probing protein interaction and function. *Nat. Commun.*, **5**, 4925.
27. Lee,S., Park,H., Kyung,T., Kim,N.Y., Kim,S., Kim,J. and Do Heo,W. (2014) Reversible protein inactivation by optogenetic trapping in cells. *Nat. Methods*, **11**, 633–636.
28. Bugaj,L.J., Choksi,A.T., Mesuda,C.K., Kane,R.S., Schaffer,D. V, Lee,S., Park,H., Kyung,T., Kim,N.Y., Kim,S. *et al.* (2013) Optogenetic protein clustering and signaling activation in mammalian cells. *Nat. Methods*, **10**, 249–252.
29. Carey,M., Kakidani,H., Leatherwood,J., Mostashari,F. and Ptashne,M. (1989) An amino-terminal fragment of GAL4 binds DNA as a dimer. *J. Mol. Biol.*, **209**, 423–432.
30. Marmorstein,R., Carey,M., Ptashne,M. and Harrison,S.C. (1992) DNA recognition by GAL4: structure of a protein-DNA complex. *Nature*, **356**, 408–414.
31. Polstein,L.R. and Gersbach,C.A. (2015) A light-inducible CRISPR-Cas9 system for control of endogenous gene activation. *Nat. Chem. Biol.*, **11**, 198–200.
32. Maeder,M.L., Linder,S.J., Cascio,V.M., Fu,Y., Ho,Q.H. and Joung,J.K. (2013) CRISPR RNA-guided activation of endogenous human genes. *Nat. Methods*, **10**, 977–979.
33. Cheng,A.W., Wang,H., Yang,H., Shi,L., Katz,Y., Theunissen,T.W., Rangarajan,S., Shivalila,C.S., Dadon,D.B. and Jaenisch,R. (2013) Multiplexed activation of endogenous genes by CRISPR-on, an RNA-guided transcriptional activator system. *Cell Res.*, **23**, 1163–1171.
34. Gilbert,L.A., Larson,M.H., Morsut,L., Liu,Z., Brar,G.A., Torres,S.E., Stern-Ginossar,N., Brandman,O., Whitehead,E.H., Doudna,J.A. *et al.* (2013) CRISPR-mediated modular RNA-guided regulation of transcription in eukaryotes. *Cell*, **154**, 442–451.
35. Ogura,E., Okuda,Y., Kondoh,H. and Kamachi,Y. (2009) Adaptation of GAL4 activators for GAL4 enhancer trapping in zebrafish. *Dev. Dyn.*, **238**, 641–655.
36. Bonger,K.M., Rakhit,R., Payumo,A.Y., Chen,J.K. and Wandless,T.J. (2014) General method for regulating protein stability with light. *ACS Chem. Biol.*, **9**, 111–115.
37. Nihongaki,Y., Yamamoto,S., Kawano,F., Suzuki,H. and Sato,M. (2015) CRISPR-Cas9-based photoactivatable transcription system. *Chem. Biol.*, **22**, 169–174.
38. Beyer,H.M., Juillot,S., Herbst,K., Samodelov,S.L., Müller,K., Schamel,W.W., Römer,W., Schäfer,E., Nagy,F., Strähle,U. *et al.* (2015) Red light-regulated reversible nuclear localization of proteins in mammalian cells and zebrafish. *ACS Synth. Biol.*, **4**, 951–958.
39. Müller,K., Engesser,R., Metzger,S., Schulz,S., Kämpf,M.M., Busacker,M., Steinberg,T., Tomakidi,P., Ehrbar,M., Nagy,F. *et al.* (2013) A red/far-red light-responsive bi-stable toggle switch to control gene expression in mammalian cells. *Nucleic Acids Res.*, **41**, e77.